Journal of Power Sources 208 (2012) 193–196

Contents lists available at SciVerse ScienceDirect

Journal of Power Sources

journal homepage: www.elsevier.com/locate/jpowsour

Short communication

High conductivity of dense tetragonal $Li_7La_3Zr_2O_{12}$

Jeff Wolfenstine [a,*], Ezhiyl Rangasamy [b], Jan L. Allen [a], Jeffrey Sakamoto [b]

[a] U.S. Army Research Laboratory, RDRL-SED-C, 2800 Powder Mill Road, Adelphi, MD 20783, United States
[b] Department of Chemical Engineering and Materials Science, Michigan State University, East Lansing, MI 48824, United States

ARTICLE INFO

Article history:
Received 12 December 2011
Received in revised form 6 February 2012
Accepted 11 February 2012
Available online 20 February 2012

Keywords:
Garnet
Tetragonal
Twins
Ionic conductivity
Hot-pressing

ABSTRACT

Hot-pressing at 1050 °C lead to near theoretical density (~98% relative density) tetragonal LLZO. The total conductivity value for dense tetragonal LLZO is $\sim 2.3 \times 10^{-5}$ S cm^{-1}. This is the highest reported value for tetragonal LLZO. This vast improvement in total conductivity is a result of the higher density achieved as a result of hot-pressing compared to conventional solid-state sintering. The value of the Li-ion lattice conductivity for dense tetragonal LLZO is 1.1×10^{-4} S cm^{-1}. The microstructure of dense tetragonal LLZO consist of twins within the grains. It is suggested that the presence of twin boundaries adds a significant contribution to the total resistance.

Published by Elsevier B.V.

1. Introduction

Presently, there is very high interest in garnet materials for use a solid-state Li-ion electrolyte in Li/Li-ion. Li-air and Li-S batteries [1–9]. To be used in these applications the garnet material must meet several requirements: high total ionic conductivity (lattice + grain boundary) and high relative density (>95%). One such garnet under consideration is $Li_7La_3Zr_2O_{12}$ (LLZO). LLZO can exhibit two structures, cubic and tetragonal at room temperature [1–11]. It has been observed in general that the cubic structure exists at room temperature when LLZO is stabilized with Al and/or Ta [1–10]. At room temperature relative densities between 93 and 98%, and total conductivity values between 1×10^{-4} and 1×10^{-3} S cm^{-1} have been reported for cubic LLZO [1–9]. In contrast the total conductivity of LLZO with the tetragonal structure has been reported to be between 1×10^{-7} and 5×10^{-6} S cm^{-1}, which is 20–10,000 times lower that that for the cubic structure [1,10,12,13]. Therefore, the reported data strongly suggests that the cubic structure is preferable for device applications. However, the previous studies which have reported on the total conductivity of tetragonal LLZO samples have had a relative density of only about 73% or less (Table 1) [12,13] and since, it is known that the total conductivity is a strong function of density, increasing with relative density [14,15], it is of scientific interest to determine the maximum total conductivity of tetragonal LLZO near its theoretical density (~100% relative density) in order to confirm the advantage of the cubic structure relative to the tetragonal structure for practical devices and further to more fully understand the structure property relationship between the two garnet structures and their Li-ion conductivities to guide future preparations of solid electrolyte materials in order to maximize conductivity.

It is the purpose of this short note to be the first to report on the total conductivity and the microstructure of tetragonal LLZO hot-pressed near to theoretical density. These results will be compared to dense cubic LLZO.

2. Experimental

2.1. Material preparation

$Li_7La_3Zr_2O_{12}$ powders were prepared from Li_2CO_3, $La(OH)_3$, "$[ZrO_2]_2{\cdot}CO_2{\cdot}xH_2O$" (zirconium carbonate, basic hydrate; equivalent ZrO_2 content determined from thermogravimetric analysis) precursor powders. The precursor powders weighed in the desired stoichiometry and then dissolved in ~1.4 M HNO_3 (aq). The resulting clear solution was evaporated to dryness in a microwave oven contained in a fume hood. Evolution of NO_x was observed during this step. The dried precipitate was lightly ground with a mortar and pestle and pressed into a pellet using a Carver laboratory die and press. The pellet was placed on a ZrO_2 plate and heated in air at 650 °C for 15 h and subsequently at 1000 °C for 4 h. The furnace was turned off and the sample was removed.

* Corresponding author. Tel.: +1 301 394 0317; fax: +1 301 394 0273.
E-mail addresses: Jeffrey.b.wolfenstine.civ@mail.mil, jwolfenstine@arl.army.mil, jeff.wolfenstine@us.army.mil (J. Wolfenstine).

0378-7753/$ – see front matter. Published by Elsevier B.V.
doi:10.1016/j.jpowsour.2012.02.031

Table 1
Conductivity and relative density data for tetragonal $Li_7La_3Zr_2O_{12}$.

Total conductivity ($S\,cm^{-1}$)	Relative density (%)	Activation energy ($eV\,atom^{-1}$)	Reference
4.2×10^{-7}	60	0.54	[13]
1.7×10^{-7}	NR	0.50 (bulk)	[2]
3.1×10^{-7}	NR	0.67	[10]
1.3×10^{-6}	77	0.43	[12]
5.2×10^{-6}	66	0.45	[12]
2.3×10^{-6}	NR	0.49	[9]
2.3×10^{-5}	98	0.41	Current study

NR = not reported.

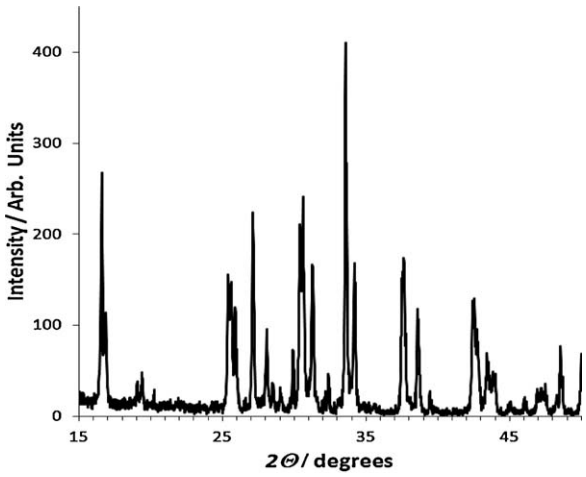

Fig. 1. X-ray pattern of tetragonal $Li_7La_3Zr_2O_{12}$.

2.2. Consolidation

A tetragonal LLZO disc was prepared by hot-pressing. The $Li_7La_3Zr_2O_{12}$ powders were hot-pressed at 1050 °C at 40 MPa pressure for 1 h under air. From the hot-pressed disc rectangular parallelepipeds were cut using a low-speed diamond saw for density, microstructural and electrical property measurements.

2.3. Property characterization

X-ray diffraction (Cu Kα radiation) was used to characterize the phase purity of the $Li_7La_3Zr_2O_{12}$ powders before and after hot-pressing. The bulk density of the hot-pressed samples was determined from the weight and physical dimensions. The relative density values were determined by dividing the bulk density by the theoretical density of tetragonal $Li_7La_3Zr_2O_{12}$ (~5.108 g cm^{-3} [13]). The microstructure of the hot-pressed sample was examined on fracture surfaces using scanning electron microscopy (SEM).

AC electrical conductivity measurements was performed on the hot-pressed sample (3 mm × 3 mm × 1 mm) using the two probe method. Au was sputter coated on to the top and bottom surfaces of the specimens. AC measurements were undertaken to determine ionic conductivity. AC impedance was measured using a Solatron 1260 Impedance Analyzer in the frequency range 1–10^6 Hz in the temperature range room temperature to 100 °C on both heating and cooling to determine the activation energy.

3. Results and discussion

The x-ray diffraction pattern for LLZO after hot-pressing is shown in Fig. 1. No second phases were observed in the x-ray diffraction pattern. The peak splitting shown in Fig. 1 is indicative of LLZO with a tetragonal structure (space group $I4_1/acd$) [13]. The x-ray pattern diffraction pattern of the calcined powder was similar to that for the bottom curve of Fig. 1, suggesting that no structural change occurred as a result of hot-pressing. The results of Fig. 1 are in agreement with results of Shimonishi et al. [1], Kumazaki et al. [2], Jin et al. [7] E. Rangasamy et al. [4], Buschman et al. [9], Geiger et al. [5], Awaka et al. [13], Il'ina et al. [12] and Logeat et al. [11], who all observed that with no impurities, either intentionally added or from contamination that only LLZO with the tetragonal structure was stable at room temperature. Rietveld refinement of the diffraction data for tetragonal LLZO using atom positions from Awaka et al. [13] yielded lattice parameters; $a = 13.077(1)$ Å and $c = 12.715(4)$ Å. These values are in rough agreement with vales of $a = 13.097$ Å and $c = 12.666$ Å [2], $a = 13.134$ Å and $c = 12.663$ Å [13] and $a = 13.1189(4)$ Å and $c = 12.6701(4)$ Å [11] for tetragonal LLZO.

The relative density of the hot-pressed tetragonal LLZO in the current study was ~98%. This value is much higher than previous investigations (~60–73%) which involved only conventional solid-state sintering. It should be noted that the conventional sintered and the hot-pressed samples were heated at nearly similar temperatures but, the additional applied stress driving force for densification during hot-pressing greatly assisted densification. As a result, the higher relative density of the tetragonal LLZO samples achieved by hot-pressing should be acceptable for Li/Li-ion solid-state, Li-air and Li-sulfur batteries whereas relative density values achieved so far by conventional solid-state sintering are not.

An SEM micrograph of the hot-pressed sample's fracture surface is shown in Fig. 2. From Fig. 2 several important points are noted. Firstly, very few voids are observed, in agreement with the high relative density measured. Secondly, the grains are fairly equiaxed with a linear intercept grain size in the range 3–10 μm. Thirdly, especially as seen in the high magnification micrograph (Fig. 2B), a banded microstructure within the grains is observed. These bands are most likely closely spaced twin platelets, similar to those observed in the ZrO_2 system, where such twins have been associated with tetragonal ZrO_2 [16–18]. None of the previous studies have reported the presence of these twins in tetrgaonal LLZO. It should be noted that in cubic LLZO no twins are observed similar, to that for cubic ZrO_2 [16,17]. Thus, the presence of such twins, which can be easily observed in the dense material, adds further confirmation to the diffraction pattern shown in Fig. 1 that undoped LLZO has a tetragonal structure at room temperature.

The room temperature AC conductivity results for the hot-pressed tetragonal LLZO sample using Li-ion blocking Au electrodes is shown in the complex impedance plot in Fig. 4. From Fig. 3 it can be seen that the data separates into a high frequency region which contains a semicircle and low frequency region which contains a spike. For this case, since we have Li blocking electrodes the spike represents a material which is predominately a Li-ion conductor with very low electronic conductivity [19–21]. The low frequency intercept of the semicircle on the Z_{re} axis gives the total ionic resistance (lattice + grain boundary) [20,21]. Using this resistance and sample dimensions the total ionic conductivity of the hot-pressed tetragonal LLZO sample was calculated. The total ionic conductivity of tetragonal LLZO is 2.3×10^{-5} S cm^{-1}. This is the highest reported value for tetragonal LLZO. It is ~5–200 times higher than previously reported vales for tetragonal LLZO (Table 1). This vast improvement in total conductivity is a result of the higher density achieved as a result of hot-pressing compared to conventional solid-state sintering. If the data for tetragonal LLZO is extrapolated to theoretical density (100% relative density) it is predicted that the maximum total conductivity value for tetragonal LLZO is ~$3–4 \times 10^{-5}$ S cm^{-1} at room temperature. This value is ~30× lower than the maximum value for cubic LLZO (~1×10^{-3} S cm^{-1}).

Assuming a general model for ionic conduction in a polycrystalline sample where the impedance spectrum shows two distinct

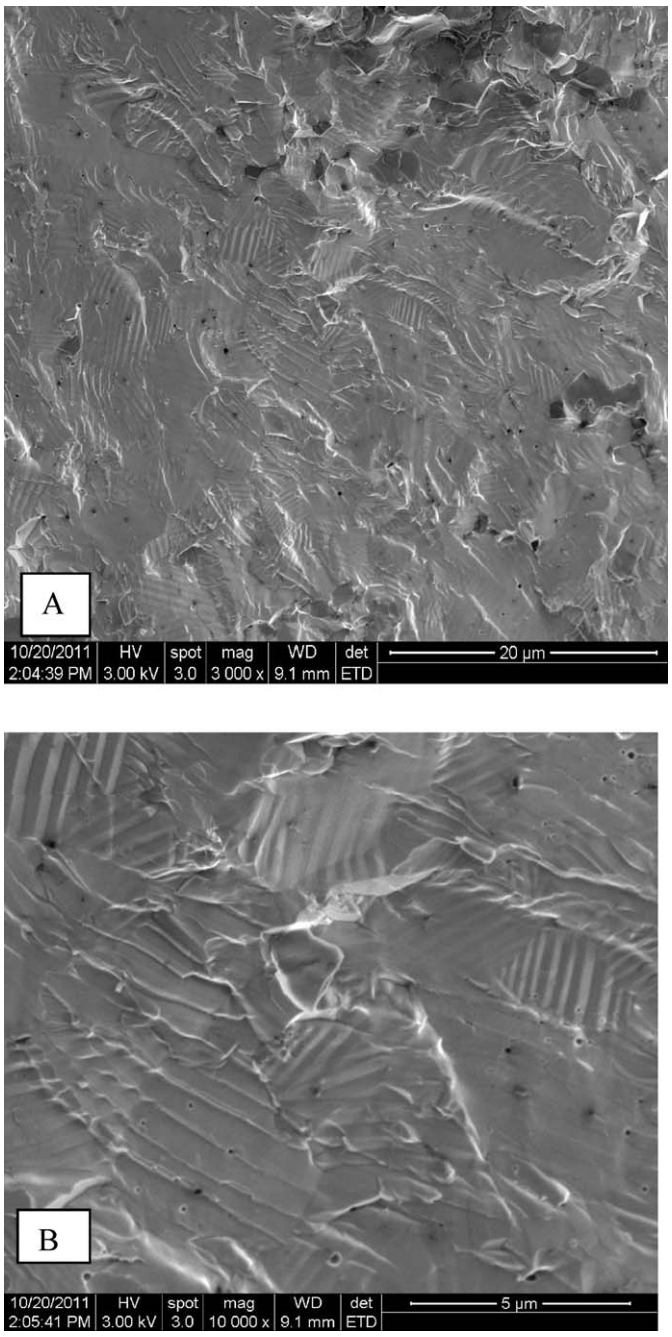

Fig. 2. SEM micrographs of dense tetragonal $Li_7La_3Zr_2O_{12}$.

semi-circle regions it is highly likely that the high frequency intercept of the semicircle on the Z_{re} axis shown in Fig. 3 gives the lattice resistance [20–23]. Using this resistance and the sample dimensions the Li-ion lattice conductivity of the dense tetragonal LLZO sample was calculated. The value of the Li-ion lattice conductivity for dense tetragonal LLZO is 1.1×10^{-4} S cm^{-1}. This value is about 100× higher than the reported value ($\sim 1.6 \times 10^{-6}$ S cm^{-1}) for lattice conductivity of tetragonal LLZO by Awaka et al. [13]. Thus, this comparison adds further confirmation that the conductivity value associated with this high frequency intercept is associated with lattice conductivity. No lattice conductivity values for tetragonal LLZO were reported by Il'ina et al. [12], Buschmann et al. [9] and Kokal et al. [10]. Reasons for the different lattice conductivity values between this study and Awaka et al. [13] are not known. However, one possible reason could be a difference in Li content between

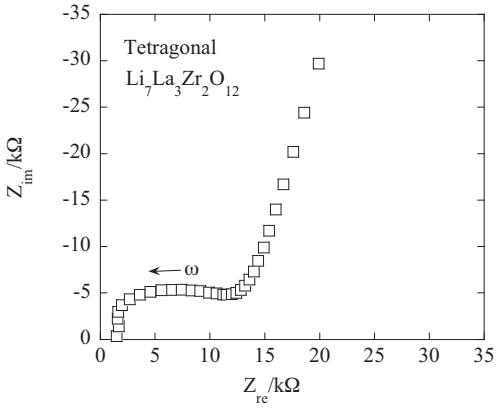

Fig. 3. Room temperature complex imdeance plot of dense tetragonal $Li_7La_3Zr_2O_{12}$.

the two studies. Furthermore, it should be noted that recent papers by Il'ina et al. [12] (5.2×10^{-6} S cm^{-1}) and Buschmann et al. [9] (2×10^{-6} S cm^{-1}) report total conductivity values higher than the lattice conductivity value reported ($\sim 1.6 \times 10^{-6}$ S cm^{-1}) for tetragonal LLZO by Awaka et al. [13]. The value (1.1×10^{-4} S cm^{-1}) for lattice conductivity for tetragonal LLZO is about 2–10 times lower than the value for lattice conductivity for cubic LLZO ($\sim 5 \times 10^{-4}$ to 1×10^{-3}) [1–8]. It is known that the difference in lattice conductivity values between the tetragonal versus cubic structure LLZO is related to Li ordering in the tetragonal structure versus Li disorder in the cubic structure [8,11,13,24,25].

The temperature dependence of the total conductivity for dense tetragonal LLZO is shown in Fig. 4. The activation energy for total conductivity (E_a) of dense tetragonal LLZO determined from the slope of curve yielded a value of $E_a \sim 0.41$ eV atom^{-1}. This value can be compared with previous values for E_a determined for the total conductivity of tetragonal LLZO, which range from 0.43 to 0.67 eV atom^{-1} (Table 1). The current value is slightly lower than the previous values, which is most likely a result of the very high relative density achieved in the present samples compared to previous studies which causes a reduced the grain boundary resistance to the total resistance resulting, in a lower activation energy for total conductivity. In contrast activation energies for total conductivity for cubic LLZO range from ~0.26 to 0.35 eV atom^{-1} [1–4,7–9]. Thus, the activation energy for total conductivity for tetragonal LLZO is higher than for cubic LLZO. An activation energy for lattice conductivity was not determined because at higher temperatures the conductivity data could not be separated into lattice and grain-boundary contributions. Awaka et al. [13], Buschman et al. [9] and Il'ina et al.

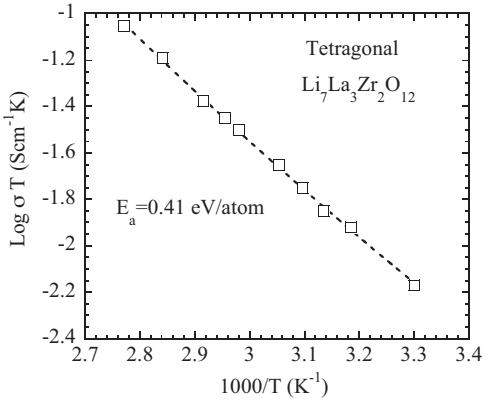

Fig. 4. Temperature dependence of the total conductivity for dense tetragonal $Li_7La_3Zr_2O_{12}$.

[12] do not report any activation energy for lattice conductivity for tetragonal LLZO.

Another interesting difference between the tetragonal and cubic LLZO at relative densities near theoretical is that the boundary contribution to the total resistance for cubic LLZO is ~10–20% [2,3,8] whereas in as seen in Fig. 3 for tetragonal LLZO it is about 80–90%. What is the source of this difference? It cannot be a result of density since; they are both being compared at near theoretical density. It most likely cannot be grain size since, the grain size for tetragonal and cubic are similar. It could be due to the difference in the structure of the grain boundaries and/or chemistries at the boundaries. This would require detailed transmission electron microscopy to prove. Another possible explanation is a result of the twins within the grains in tetragonal LLZO compared to cubic LLZO where no twins are present. It has been shown that the presence of twin boundaries within single crystalline $Li_3Fe_2(PO_4)_3$ can increase the total resistance compared to the same single crystal without twins [26]. Thus, it is highly possible that twin boundaries within the grains can add a significant contribution to the total boundary resistance. Hence, it is expected that for tetragonal LLZO which contain twins within the grains that the ratio of total boundary contribution to the total resistance will be higher than in cubic LLZO where no twins exist. This suggestion is in agreement with data in the literature and the results of Fig. 3. To confirm this suggestion would require very high-resolution impedance spectroscopy or vary the number of twin boundaries within the grains and observe this effect on conductivity.

The results of this study reveal for dense (close to theoretical density) tetragonal LLZO that the total conductivity is lower and the activation energy is higher compared to dense cubic LLZO. The microstructure of dense tetragonal LLZO consists of twins within the grains whereas none are observed in cubic LLZO. The presence of these twin boundaries adds a significant contribution to the total resistance.

4. Conclusions

Hot-pressing at 1050 °C can lead to near theoretical density (~98% relative density) tetragonal LLZO. In contrast previous investigations using conventional solid-state sintering have achieved a maximum relative density of only ~77%. The total conductivity value for dense tetragonal LLZO is $\sim 2.3 \times 10^{-5}$ S cm^{-1}. This is the highest reported value for tetragonal LLZO. This vast improvement in total conductivity is a result of the higher density achieved as a result of hot-pressing compared to conventional solid-state sintering. The activation energy for total conductivity (~0.41 eV atom^{-1}) is in agreement with literature values for tetragonal LLZO. The results of this study reveal for dense (close to theoretical density) tetragonal LLZO that the total conductivity is lower and the activation energy is higher compared to dense cubic LLZO. The microstructure of dense tetragonal LLZO consist of twins within the grains whereas none are observed in cubic LLZO. It is suggested that the presence of twin boundaries adds a significant contribution to the total resistance.

Acknowledgements

JW and JAL would like to acknowledge support of the U.S. Army Research Laboratory (ARL). JS would like to acknowledge the support of the U.S. Army Research Office (ARO).

References

[1] H. Shimonishi, A. Toda, T. Zhang, A. Hirano, N. Imanishi, N. Yamamoto, Y. Takeda, Solid State Ionics 183 (2011) 48.
[2] S. Kumazaki, Y. Iriyama, K.H. Kim, R. Murugan, K. Tanabe, K. Yammato, T.T. Hirayama, Z. Ogumi, Electrochem. Commun. 13 (2011) 509.
[3] R. Murugan, V. Thangaduri, W. Weppner, Angew. Chem. Int. Ed. 46 (2007) 7778.
[4] E. Rangasamy, J. Wolfenstine, J. Sakamoto, Solid State Ionics 206 (2012) 28.
[5] C.A. Geiger, E. Alekseev, B. Lazic, M. Fisch, T. Armbruster, R. Langner, M. Fechtelkord, N. Kim, T. Pettke, W. Weppner, Inorg. Chem. 50 (2011) 1089.
[6] M. Kotobuki, H. Munakata, K. Kanamura, Y. Sato, T. Yoshida, J. Power Sources 196 (2011) 7750.
[7] Y. Jin, P.J. McGinn, J. Power Sources 196 (2011) 8683.
[8] Y. Li, C.A. Wang, H. Xi, J. Cheng, J.B. Goodenough, Electrochem. Commun. 13 (2011) 1289.
[9] H. Buschmann, J. Dolle, S. Berendts, A. Kuhn, P. Bottke, M. Wilkening, P. Heitjans, A. Senyshen, H. Ehrenberg, A. Lotnyk, V. Duppel, L. Kienle, J. Janek, Phys. Chem. Chem. Phys. 13 (2011) 19378.
[10] I. Kokal, M. Somer, P.H.L. Nooton, Solid State Ionics 185 (2011) 42.
[11] A. Logeat, T. Kohler, U. Eisele, B. Stiaszny, A. Harzer, M. Tovar, A. Senyshyn, H. Ehreberg, B. Kozinsky, Solid State Ionics 206 (2012) 33.
[12] E.A. Il'ina, O.L. Andreev, B.D. Antonov, N.N. Batalov, J. Power Sources 201 (2012) 169.
[13] J. Awaka, N. Kijiama, H. Hayakawa, J. Akimoto, J. Solid State Chem. 182 (2009) 2046.
[14] H. Aono, E. Sugimoto, Y. Sadaoka, N. Imanaka, G.-y. Adachi, J. Electrochem. Soc. 137 (1990) 1023.
[15] J. Wolfenstine, J.L. Allen, J. Read, J. Sakamoto, G. Gonzalez-Doncel, J. Power Sources 195 (2010) 4124.
[16] T.-S. Seu, T.-Y. Tien, I.-W. Chen, J. Am. Ceram. Soc. 75 (1992) 1108.
[17] J. Sakuama, Y.-I. Yoshizawa, H. Suto, J. Mater. Sci. 20 (1985) 2399.
[18] M.S. Yanagisawa, M. Kato, H. Seto, N. Ishizawa, N. Mizutani, M. Kato, J. Am. Ceram. Soc. 70 (1987) 503.
[19] J. Jamnik, J. Maier, J. Electrochem. Soc. 146 (1999) 4183.
[20] R.A. Huggins, Ionics 8 (2002) 300.
[21] J.E. Baurle, J. Phys. Chem. Solids 30 (1969) 2657.
[22] P.G. Bruce, A.R. West, J. Electrochem. Soc. 130 (1983) 662.
[23] L.C. De Jonge, J. Mater. Sci. 14 (1979) 33.
[24] E.J. Cussen, J. Mater. Chem. 20 (2010) 5167.
[25] J. Percival, E. Kendrick, R.I. Smith, P.R. Slater, Dalton Trans. (2009) 5167.
[26] A.K. Ivanov-Schitz, J. Schoonman, Solid State Ionics 91 (1996) 93.